ISSN 2277-2685
IJESR/April. 2026/ Vol-16/Issue-2s /27-38
Rabiya Begum *et. al.*, / International Journal of Engineering & Science Research
Full Length Article

A Survey of Dual-Axis Solar Tracker System Using Arduino PHASE-II

Rabiya Begum[1], Md. Uzma Begum [2], Shaik Abdul Gaffur [3]
Dr Syeda Gauhar Fatima[4], Mr. V A Imran[5],
UG student[1,2,3], Professor[4], Associate Professor[5]
Department of Electronics and Communication Engineering Deccan college of engineering and technology, Hyderabad, Telangana, India
Accepted 23-04-2026

Abstract:
This paper describes the design and implementation of an energy efficient solar tracking system from a normal mechanical single axis to a hybrid dual axis. For optimizing the solar tracking mechanism electromechanical systems were evolved through implementation of different evolutional algorithms and methodologies. To present the tracker, a hybrid dual-axis solar tracking system is designed, built, and tested based on both the solar map and light sensor based continuous tracking mechanism. These light sensors also compare the darkness and cloudy and sunny conditions assisting dailytracking. The designed tracker can track sun's apparent position at different months and seasons; thereby the electrical controlling device requires a real time clock device for guiding the tracking system in seeking solar position for the seasonal motion, So the combination of both of these tracking mechanisms made the designed tracker a hybrid one. The power gain and system power consumption are compared with a static and continuous dual axis solar tracking system. It is found that power gain of hybrid dual axis solar tracking system is almost equal to continuous dual axis solar tracking system, whereas the power saved in system operation by the hybrid tracker is 44.44% compared to the continuous tracking system 'A dual-axis solar tracking system with a novel and simple structure was designed and constructed, as documented in this paper. The photoelectric method was utilized to perform the tracking. The solar radiation values of the designed system and a fixed panel system were theoretically estimated and compared, showing that the proposed system is more efficient in collecting solar energy than a fixed solar panel with a 30° tilted fixed surface facing south. The experimental results verified the validity of the prediction as well as the efficiency of the proposed solar tracking system. In a comparison of the data obtained from the measurements, 24.6% more energy was seen to have been obtained in the dual-axis solar tracking system compared to the fixed system. This study possesses potential value in small- and medium-sized photovoltaic applications.

1. Introduction

Due to the already high and constantly increasing demand for energy worldwide, the exploitation of various conventional energy sources has been induced. Considering the environmental issues that non-renewable energy sources cause—for instance, the emission of greenhouse gases—renewable sources of energy such as solar, wind, biomass and hydro have been adopted to limit and reduce this degradation. Among these, solar energy holds significant promis, as it is one of the most abundant, clean, cost-free and inexhaustible resources of energy. To convert solar energy into electrical energy, Photovoltaic Voltage (PV) solar panels have been widely used as important components of solar tracking systems. A PV solar panel comprises a large number of solar cells composed of silicon-like semiconductors. It works by transferring the energy of photons from sunlight that strikes the solar cells to silicon electrons, which then flow through electrodes and the external circuit and generate an electric current.

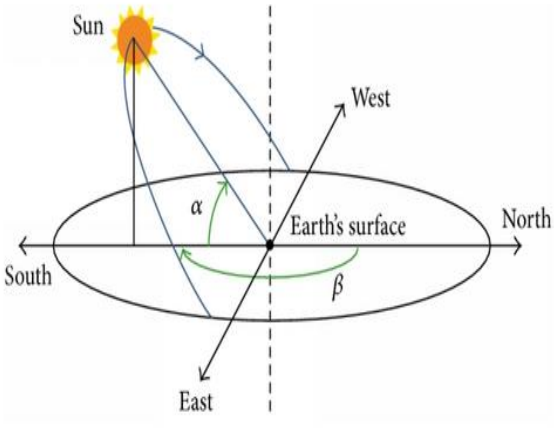

Fixed solar panels have been utilized over the past few decades since fixed tracking can easily accommodate harsh environmental conditions. There are three typical structural installations for fixed solar panels: namely, fixed-angle, vertical and season-adjusted fixed-angle installations. Fixed-angle solar panels have been extensively applied in large solar power stations and rooftop solar tracking systems, while vertical panels are available for vertical structures with limited space, such as the façades of high-rise buildings. With season-adjusted fixed-angle systems, the solar panels' tilt angles in the horizontal direction can be modified for seasonal variations in order to maximize the collected amount of solar radiation. Nevertheless, angle adjustment is not that convenient due to many site attributes, such as security measures for working on rooftops or other high buildings and the human cost of adjusting a large number of solar panels in solar power stations.Compared to fixed solar panels, solar tracking systems that can track the position of the sun based on both the season and the moment of each day have higher solar energy collection efficiency, thus possessing broader applications and higher research value. Based on the different degrees of freedom of structures, there are two different types of solar tracking systems: single-axis and dual-axis. The former is designed to track the sun on a single axis according to the azimuth angle, while the latter is designed to track it via dual axes corresponding to the azimuth and solar altitude angles. In recent years novel, technologies and designs for both types have been developed to achieve high control accuracy and structural reliability for these systems' practical performance.

Literature review

The first solar tracker was a mechanical system by C. Finster, invented in 1962. Though the Finster solar tracker realized insignificant energy gains, years of testing and research have led to improvement of the conversion output of the PV system and consequently the emergency of different tracking technologies and applications (e.g. concentrator and non-concentrator). In short, improved solar cells have been developed and the use of solar tracking system over the use of conventional fixed PV system has grown. In fixed photovoltaic system the solar receiver (PV module) is in a stationary position facing the true north. However, with mechanical or electro-mechanical systems, the orientation of the collect change continually in reference to the azimuthal directions (east-west) and also in its elevation. This is dependent on the tracker's geometrical capacity. 2.1. Classification of solar tracking system Mousazadeh et al, (2009) carried a review study, which resulted in the general categorization of solar tracking systems according to two main typologies, namely, Energy source (i.e. passive, active and manual), and Degree of freedom (i.e. single or dual axis). Passive tracking systems- designate all devices that position solar collectors for optimum capture of energy using mechanical potential and thermal energy principles.

Shape Memory Alloy (SMA), Thermo-fluids, Mechanical potential system (lever, weight and springs). In Shape Memory Alloy, cylindrical actuators to change the shape the SMA receivers through mirrors until an optimum orientation is achieved Recent developments, among others by Kuser et al (2015), have seen the use of high-pressure fluids to convert the potential energy in the mechanical structure that hold up the PV panel into kinetic energy, which is then used to move the panel toward the sun.

Active tracking systems- use electrical energy as their source. A number of categories exist such as; Electro-optical based tracker, Auxiliary bifacial solar cell and chronological (time and date based) tracker. At some instances, a combination of these different systems may be realized and the resulting system will be referred to as Hybrid. Of all active trackers, electro-optical based trackers are is generally more popular. Mousazadeh et al (2009) reports the use of differential illumination of coupled electro sensors to generate a differential signal to a controller which then sends a signal to drive the solar system. For improved photosensitivity, the sensor can be mounted on a pyramidal structure (in the figure 2b outlines the photo-diode mounted on pyramid) or use of collimator tube might be vital as it prevent diffuse irradiation from reach the sensors therefore ensuring precise measurement of the position of the sun. a system made up of four mini-solar module positioned on the North-south and east-west that detect the light intensity, this is system also use the Programmable Logic Controller (PLC) manipulate the two positioning mechanism through two DC motors, Different configuration of Photo-sensor used for active tracking mechanism, Auxiliary Bifacial Solar cell tracker- In this type of trackers an auxiliary PV cell is used to sense the position of sun and also provide the tracking energy, as it is connected to a permanent magnet DC motor. Both these are fixed to a driving axle of the tracker.

Design and Implementation Process

The whole work involves the reading of different sensor values and then comparing them digitally to determine the exact position of the sun in east-west direction. Again the system is also given some predefined values based on the sun's geographical location in the north-south direction. Overall the entire system can intelligently track the sun's movement

both in horizontal and vertical axis. In order to simplify the design and implementation process the whole system is divided into two parts.

These are as follows:

(A)mechanical system design;

(B)electrical circuit design.

(A) Mechanical System Design. Assembling the mechanical system was the most challenging part of this system because the objective was to make an energy efficient solar tracking system which demanded intelligent operations of the tracking motors. Generally, one of these motors is used for daily tracking (east-west motion) and other for making a seasonal tracking (north-south motion). So, the daily tracking motor operates continuously

based on light sensors and the annual motion tracking motor operates only a few times over the year. So, for design and implementation process the whole mechanical system is mainly divided into three parts as follows:

1. linear actuator;
2.panel carrier
3. panel carrier rotator.

1.Linear Actuato:. A linear actuator converts circular motion to a linear vertical motion in contrast to the circular motion of a conventional electric motor. The linear vertical motion is used for creating the seasonal angle of the sun. In this tracking system linear actuator consists of one stepper motor, screw thread, bolt, bearing, circular rod, and some pieces of wood.Experimentally it is found that this mechanical structure has a special feature of high weight lifting using a low power stepper motor.

Linear actuator gives the linear motion in vertical axis (upward and downward) and is connected to one end of panel carrier through a straight single rod hook. The rod hook is attached to the wooden frame. There are some bolts and these are tied with seven 15-inch-long circular rods of 2mm diameter. There is also a 13-inch-long screw thread and its diameter is 6mm. A bolt is attached in the middle of the wooden frame and this bolt is also tied with the screw thread. Four circular rods are also mortised through the wooden frame.

The wooden frame moves up and down along with the bolt and the single rod hook. It works in such a way that the wooden frame does not let the bolt move along with the thread screw rather when the thread screw moves then the four circular rods mortised into the wooden frame cause the bolt to move up or down. Now when the single rod hook moves upward or downward it moves along with the panel carrier. The two ends of screw thread are placed in two bearings which helps it to rotate smoothly. These bearings are mortised into the roof and floor. One gear is also placed at the bottom of the screw thread and this gear is connected to the stepper motor gear which is placed on the floor of the linear actuator body. The floor and roof of the linear actuator are made of wood which holds all the linear actuator instruments.

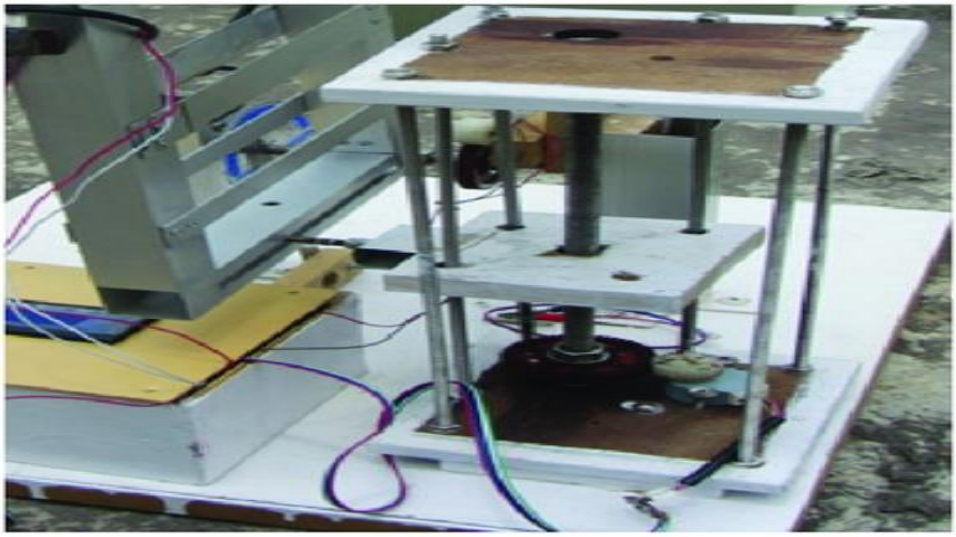

Panel Carrier. Panel carrier is basically a rectangular frame made of aluminum which holds the solar panel with the help of a circular rod. One end of the horizontal base of the panel carrier is attached with the single rod hook of linear actuator and other with the panel carrier rotator. A stepper motor with a gear is placed on the body of the aluminum frame. When the stepper motor rotates along with its gear then the panel rotates from east to west by tracking sun's daily motion active

2. 2. EFFICIENCY TRAJECTORY OF PV

OUTPUT DUE TO DUAL AXIS TRACKERS OVER THE PAST TWO DECADE

In1997 Hoffmann, R., et al. reported an efficiency improve of more than 30% on an open loop active tracker which was evaluated on PV concentrators. In 1998 an experimental review of closed loop active tracker, with solar cell used to sensor the position of the sun result in improvement of efficiency 30-50%. The tracking was tested in northern regions of Chile. Yousef. (1999) developed a tracker that deployed an artificial intelligence approach. A PC based fuzzy logic control, which acquired data through photo-diode to drive motors was engaged, the system increased conversion efficiency of PV system by 50%. A study on performance of different tracking configuration carried out in Germany outlined a 30% increase due to active tracker. Dougherty, B. (2001) describes a mobile tracking device with was part of Building Integrated PV testing facility achieved 40% conversion efficiency over fixed. A field tested (in Malta) auxiliary PV cell based, roof mounted tracking system recorded a 40% efficiency increase. A tracker used in water pumping is reported to efficiency increase of 19-24%. Abdallah, S. and Nijmeh, S. (2004) Carried out experimental evaluation on a PLC deployed in a real time-based tracking system in Jordan. The authors found a 41.34% increase of efficiency. In 2005 Piao, Z.G., et al developed and conducted laboratory test for a time-based active tracker, which used a micro-controller and engaged idle mode in gloomy sky conditions. Furthermore a 21% efficiency increase was reported.

Experimentally tested tracking system in Jordan by Mamlook, et al., (2006) achieved efficiency improvement of 40%. This tracker was a solar mathematical formula based with a PLC. Rubio, F., et al., (2007) developed and experimentally tested a PC controlled through mathematical formulae with PV arrays used as feedback sensors. SCADA used for supervision and monitoring with an application developed in LABVIEW. The system attained a 40% efficiency over fixed PV collector. Chen-Sheng, et al., (2008) repots a 49.2% increase in efficiency due to a system, developed and filed tested in Tibet. The tracker was developed to deploy a Microprocessor as a controller, (time-based system with feedback from position sensors). Also, it had a poor environment protection (Wind, Vibrations and cloud) and human - machine interface. In 2009 Cemil Sungur recorded 42.6% efficiency improved after experimentally testing a real time based, PLC controlled and DC motor driven tracker in Turkey. Barsoum, N. and Vasant, P., (2010) achieved 40% efficiency improvement over fixed through a microcontroller (PIC16F84A), LDRs and DC Motor based tracker. A Micro-controller was used for multi-function approach tracking, by Kassem, A. and Hamad M. (2011) achieved a 64%. In 2012 Eke, R. and Senturk, A., evaluated a commercial (in Turkey) Pesos SF-40SD dual axis tracking mounted on Mono Crystalline silicon PV and found a 30.79% increase in efficiency. Anusha, K. and Chandra Mohan Reddy's. (2013) realized a 40% increase due to a system real time based, which deployed Microcontroller (LPC2148) and Stepper Motor. Singh, K.P., and Gupta, B., (2014) Experimental (India) Microcontroller (P1C16F877A programmed in DOTNET), Stepper Motor geared (Worm and spur) Infra-red sensor 35-42% (26). In 2015 Ceyda, A.T., and Cenk, Y., (2015) evaluated a microcontroller (PIC16F877A programmed in MPLAB IDE) with linear actuators and potentiometer (feedback sensors) based tracking system at laboratory scale in Turkey. In this study efficiency of 40% was recorded. A Microcontroller (At mega 8), LDRs, DC motor geared and L293D motor driver was also constructed and tested at experimental scale by Shashwati, R. and Tripathi, A.K (2016) and 40% efficiency was realized. Akbar, H.S., et al., (2017) developed a microcontroller (At mega 328), LDRs, DC motors and relays. Through the system efficiency of about 55-30% was recorded.

Structural Design and Operational Principles of the Solar Tracking System

The mechanical structure of the system, shown in Figure 1, includes solar panel components, gears, support members, power storage units, photodiodes and control modules. In this solar tracking device, a Microcontroller Unit (MCU) is the core controller that analyzes the signals transmitted from each component and controls the motor to rotate the solar panel to the appropriate angle. Photoresistors on the boundaries of the solar panel are used to adjust the device. The battery stores power transferred from solar energy and supplies it to the control modules and the dynamic devices.

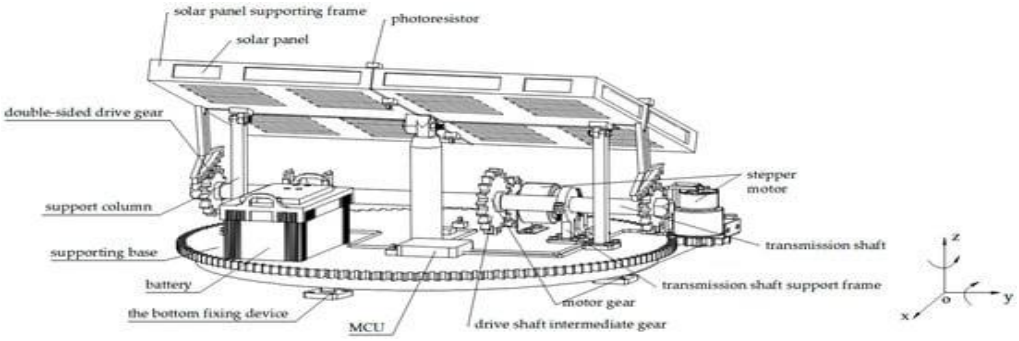

Figure 1. Structure diagram of the solar tracking device.

For dual-axis solar tracking performance, the structure in Figure 1 should have the ability to rotate in the east–west and south–north directions. The components that fulfill this rotation can be seen in Figure 2. For the rotation of the solar panel in the east–west direction, the supporting base is driven by a motor gear. A diagram of its bottom is depicted in Figure 2a, illustrating that the bottommost fixed device is placed on the ground and linked by a supporting base and pins. In the center of the supporting base, there is a base bearing. The stepping motor can lead to the rotation of the base via driving the motor gear, thus inducing the east–west rotation of the solar panel on the base, namely, the rotation in the plane xOy. For the south–north rotation of the solar panel, i.e., the rotation in the plane xOz, the stepping motor can trigger the rotation of the solar panel's supporting frame by driving the rotations of the motor gear, the intermediate drive shaft gear, the transmission shaft and the double-sided drive gears (see Figure 2b). Accordingly, the rotations of the panel in both directions are independent of each other.

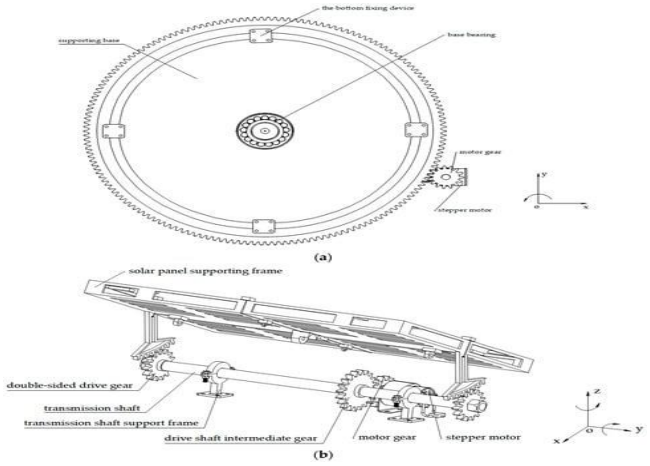

Figure 2. Components to perform rotation in two directions: (**a**) east–west and (**b**) north–south

As shown in Figure 2, for the spur gears to perform the rotation, a 20° pressure angle was set, as it is the preference of most designers. The solar panel was set to be a rectangular shape with a length of 840 mm, a width of 600 mm and a thickness of 20 mm. Considering the stability of the base of the solar panel, the pitch diameter of the base gear was set to nearly the diagonal length of the solar panel, namely, $dpb = 996mm$. Since the most common module for spur gears is 6 mm, we set the module for the gears of this device at M = 6 mm. The number of teeth on the base gear can be calculated as $N1 = \frac{dpb}{M} = 166$. For the motor gear meshed with the base gear, we used the dimension of the pitch diameter, $dpm = 90mm$; thus, the number of teeth is $N2 = 15$. On this basis, in Figure 2b, the gear ratio is $mG1 = \frac{N1}{N2} = 11.07$, and the dimensions of the gears are used as follows: the pitch diameter of the driving shaft intermediate gear, $dpb = 120mm$, and the number of teeth, $N3 = 20$; the pitch diameter of the double-sided drive gears being the same as that of the motor gear in Figure 2a,

i.e.,$dpb = 90mm$, and the number of teeth of each gear, $N2 = 15$; and the pitch diameter of the transmission shaft on the solar panel supporting frame$dpt = 462mm$, and its number of teeth, $N4 = 77$. From the gear ratio in Figure 2b, the following can be concluded:

$$m_{G2} = \frac{d_{ps}\, d_{pt}}{d_{pm}^2} = \frac{N_3\, N_4}{N_2^2} = 6.84. \quad (1)$$

We then applied the photoelectric method [31] of solar tracking. This method depends on the outputs of the photoresistors on the edges of the solar panel, as shown in Figure 1. Here, we note the signals of the photoresistors on the upper, lower, right and left edges with the coefficients m1, m2, m3 and m4, respectively. The route of the photoelectric tracking method of the designed structure is displayed in Figure 3. m1 and m2 were converted into digital signals with an Analog/Digital (A/D) conversion circuit and transferred to the MCU,whichthen induced the rotation of the stepping motor so as to lead to the rotation of the solar panel's supporting frame, as shown in Figure 2b. This process is for the panel adjustment of the rotation in the south–west direction, which would not stop until the values of m1 and m2 were equal. Considering that this solar tracking system is sensitive to practical weather disturbances such as clouds and shadows, we set the equality of m1 and m2 to meanthat m1 was within the range of 97.5% to 102.5% of m2. A tolerance range of ±2.5% was adequate for this application. For the adjustment of the rotation in the east–west direction, the process was similar; the deterministic parameters were m3 and m4. The solar tracking was completed when the adjustment in the two directions was finished

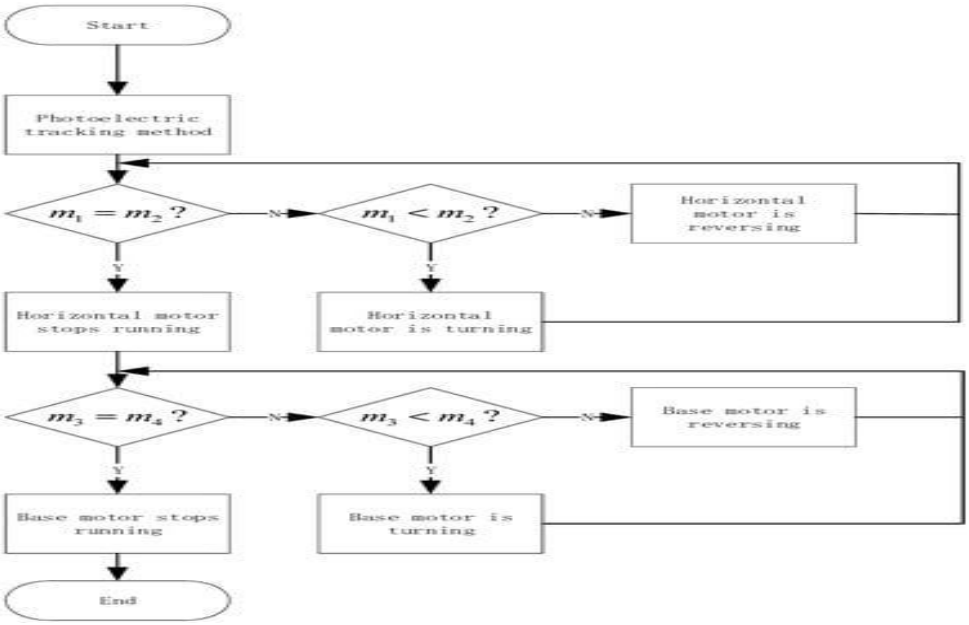

Figure 3. Control algorithm of the solar tracking system

Energy Harvesting Efficiency Analysis

On the basis of the photoelectric tracking method, we analytically evaluated and compared the total radiation of the solar panels of the designed and fixed systems in the same location and with the same weather. To this end, formulas to determine the relevant parameters, such as time, declination angle, day length, hour angle and ratio of hourly radiation, were expressed at first.

We adopted the time parameter reported in Ref. The Equation of Time (EoT) for each day of the year is expressed as:

$$EoT(N) = 9.87\sin(2B) - 7.53\cos(B) - 1.5\sin(B), \quad (2)$$

Where

$$B = \frac{360(N-81)}{364}, \quad (3)$$

and N is the day number. For instance, on 1 January, N =1.

The corresponding declination angle in degrees is

expressed as the following formula:

$$\delta = 23.45 \sin\left(\frac{360(284+N)}{365}\right), \quad (4)$$

Based upon this, the hour angle at sunset and the length of the day in hours can be expressed as follows:

$$h_{ss} = arccos(-\tan(L)\tan(\delta)), \quad D\iota = -\frac{2}{15}\tan(L)\tan(\delta), \quad (5)$$

Respectively. Here, the parameter L represents the local latitude. Since the time intervals between noon and sunrise/sunset are equal, the following number,n, was introduced to note the time intervalin hours:

$$n = \left[\frac{D\iota}{2}\right], \quad (6)$$

Within each time intervel, namely, the number of the exact ranges from 1 to n, the angle for each hour can be expressed as:

$$h\iota = 15°(LST + EoT(N) + 4(SL - LL) - 12) \quad i = 1\ldots n, \quad (7)$$

Where LST means local standard time, SL means standard longitude and LL means local longitude. The plus and minus signs in equation(7) correspond to cases of afternoon hours and morning hours, respectively. The solar incidence angle, θι, in each hour, depending on the location of the solar panel,is expressed as:

$$\theta\iota = arccos(\sin + (L\beta o)\sin(\delta) + \cos(L + \beta o)\cos(\delta)\cos(h\iota)) \quad i = 1\ldots n, \quad (8)$$

Where βo is the tilt angle of the fixed solar surface from the horizontal plane, and the plus and minus signs apply to the locations of the solar panel in the northern and southern hemispheres, respectively.

Thus, the ratio of hourly to daily total radiation can be written as:

$$ri = \frac{15\pi(a+b\cos(h_i^+))(\cos(h_i^+) - \cos(h_{ss}))}{360\sin(h_{ss}) - 2\pi h_{ss}\cos(h_{ss})} \quad i = 1\ldots n, \quad (9)$$

Where

$$a = 0.409 + 0.5016\sin(hss - 60°), b = 0.6609 - 0.4767\sin(hss - 60°), \quad (10)$$

On this basis, the energy collected by the stationary solar tracking system for the whole day can be obtained as follows:

$$W_{fixed} = HS\eta\sum_{i=1}^{n} r_i\cos(\theta i). \quad (11)$$

In the above equation, the parameters H, S and η represent the daily solar irradiation per unit area, the solar panel area and the energy conversion efficiency of the solar panel, respectively. Here, it is worth mentioning that the case for $\cos\theta i < 0$ does not mean the dissipation of solar energy via the solar panel; instead, it indicates that the sun is behind the solar panel and, thus, no solar energy can be harvested. Therefore, when $\cos\theta i < 0$, we set $\cos\theta i = 0$ in Equation (11). In most of the daylight hours, for the fixed panel, $\theta i \neq 0$, namely, $\cos\theta i < 1$.

.

For differences in the solar tracking system with the same solar panel and under the same weather conditions, since the solar tracker keeps the solar panel perpendicular to the solar radiation during daylight hours, $\cos\theta i = 1$. As the sum of the ratio, ri , for a whole day, $\sum_{i=1}^{n} ri = 1$. The collected energy of the solar tracking system for the same day would be:

$$W_{tracked} = HS\eta, \quad (12)$$

Obviously,$Wtracked > Wfixed$.

Taking the location at the30.8466° latitude and 121.5164°longitude in Shanghai, China, as an example, the exact period we considered was five days long, from 27 March 2023, to 31 March 2023. Assuming sunny weather, we calculated the approximate collected energy of the solar panels

of the fixed solar panel and the proposed solar tracking system. The values of some related parameters are provided in Table 1.

Table 1. Parameter table of values for calculation.

In substituting the values of the parameters in the above table in Equations (11) and (12) and noting the average collected energy of the five days as:

$$\widetilde{W}_{fixed} = \frac{1}{5}\sum_{N=86}^{90} W_{fixed}^{N}, \quad \widetilde{W}_{tracked} = \frac{1}{5}\sum_{N=86}^{90} W_{tracked}^{N}, \quad (13)$$

We obtained

$$\frac{\widetilde{W}_{tracked}\widetilde{W}_{fixed}}{\widetilde{W}_{fixed}} \approx 26.7\%, \quad (14)$$

implying that ideally, the energy collected via the designed solar tracking system would be much higher than that of the fixed solar panel on a daily basis.

Whether the designed solar tracking system can be more efficient in energy harvesting than the fixed system depends on not only the extra energy collected but also the energy consumption required to control and drive the solar panel rotation in each system. Expressing $\widetilde{W}tracked$ as the average power of the solar panel, Psp, and the length of the day, $D\imath$, and substituting their form into Equation (14) yielded:

$$\widetilde{W}_{tracked} = D_i P_{sp}, \quad (15)$$

And

$$W_{extra} = \widetilde{W}_{tracked} - \widetilde{W}_{fixed} = 0.2111 D_i P_{sp}. \quad (16)$$

Next, we applied two stepping motors to the designed system. Every half hour, the selected motors could work for 30 s, hence operating up to 4n times per day. Their working period for each time is $tm = \frac{1}{120}$.Considering that the stepping motor operates at full power and the total power consumption of the sensors and other control modules is negligible relative to the energy consumption of the motor, the energy consumption of the stepping motor can be written as:

$$W_{consume} = 8nt_m P_m = \frac{[D\imath]}{30} P_m \quad (17)$$

since the designed structure is lightweight with typical materials, the power of the motor to drive the rotation, P_m, can be less than P_{sp}. Comparing the extra collected energy, $Wextra$, and the consumed energy of the device, $W_{consume}$, yields:

$$\frac{W_{extra}}{W_{consume}} = \frac{6.333 P_{sp}}{P_m} >> 1. \quad (18)$$

It follows that the increase in collected energy when the proposed solar tracking device is used to replace the fixed one can be far greater than the energy consumed in driving the designed device, demonstrating the energy-harvesting efficiency of the designed system.

Experimentation and Results

In this section, experimental measurements are documented to verify the validity of our analysis as well as the efficiency increase for solar energy with the designed solar tracking system. A continuous test was carried out for 5 days, from 27 March to 31 March, at the Shanghai Institute of Technology, Shanghai, China. The location of this test was in Southeast China, at the latitude and longitude illustrated in Table 1. The outdoor temperature ranged from 9 °C to 20 °C. Pictures of the prototype of the designed solar tracker and the stationary solar panel are provided in Figure

4. Here, the dimensions of the prototype depicted in Figure 4a were one-tenth of the dimensions of the numerical model shown in Figure 1. The two solar panels, made of polysilicon, had the same-sized rectangular shape, with a length of 84 mm, a width of 60 mm and a thickness of 2 mm. Their maximum open-loop voltage was 6.3 V. The supporting base of the structure was made of polymethylmethacrylate (PMMA) plastics, and the double-sided drive gears, the motor gear, the support columns and the support frame of the solar panel were all made of polyoxymethylene (POM) plastics. We selected a 28BYJ-48 stepping motor with a working voltage range of 5 V–12 V and a step angle of $\frac{1}{64}°$, as well as an STC89C 52 MCU with a working voltage of 3.3 V and photoresistors with a light resistance range of $2k\Omega - 5k\Omega$ and a dark resistance of $200k\Omega$. The fixed-surface solar panel, tilted at 30° toward the south with the same-sized solar panel, is presented in Figure 4b.

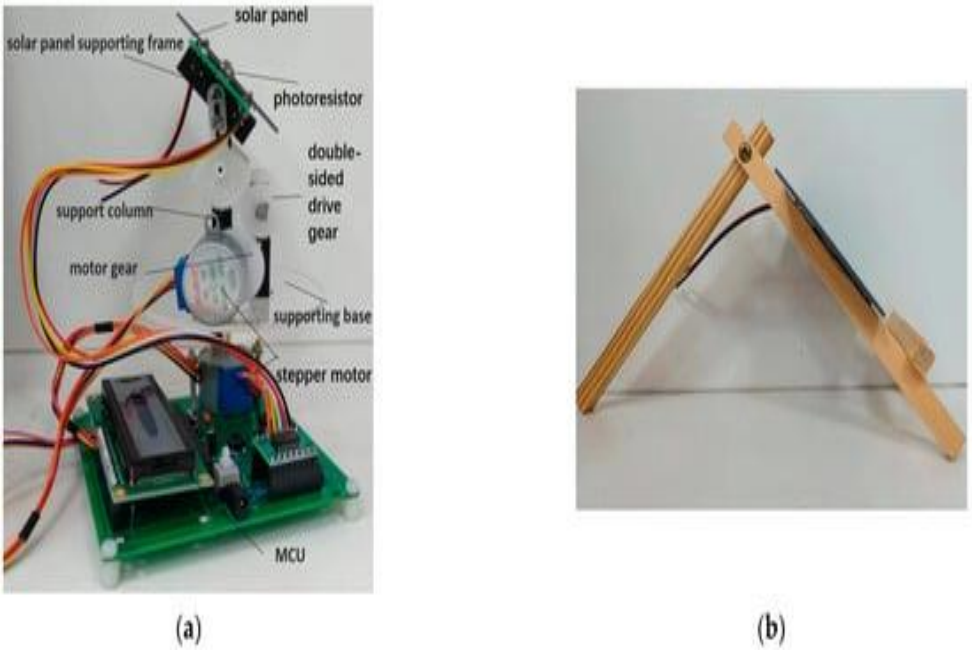

Figure 4. Installation of two solar panels: (a) tracking prototype and (b) fixed panel

Based on Equation (6), we calculated that from 27 March to 31 March 2023, the day lengths in hours were 12.16, 12.19, 12.22, 12.26 and 12.29, respectively. The average number of daylight hours was 12.22. For the convenience of measurement and calculation, we set the daytime for each day in the experimental period at 12 h: namely, from 6 a.m. to 6 p.m. Hence, we collected the average solar radiation power values of the two panels for each hour, measured from 6 a.m. to 6 p.m., as shown in Figure 6. The energy power of the solar tracking device was observed to be higher than that of the fixed panel during the daytime. Additionally, the solar radiation power of the two panels both increased from 6 a.m. to noon, i.e., 12 p.m., but decreased from 12 p.m. to 6 p.m.

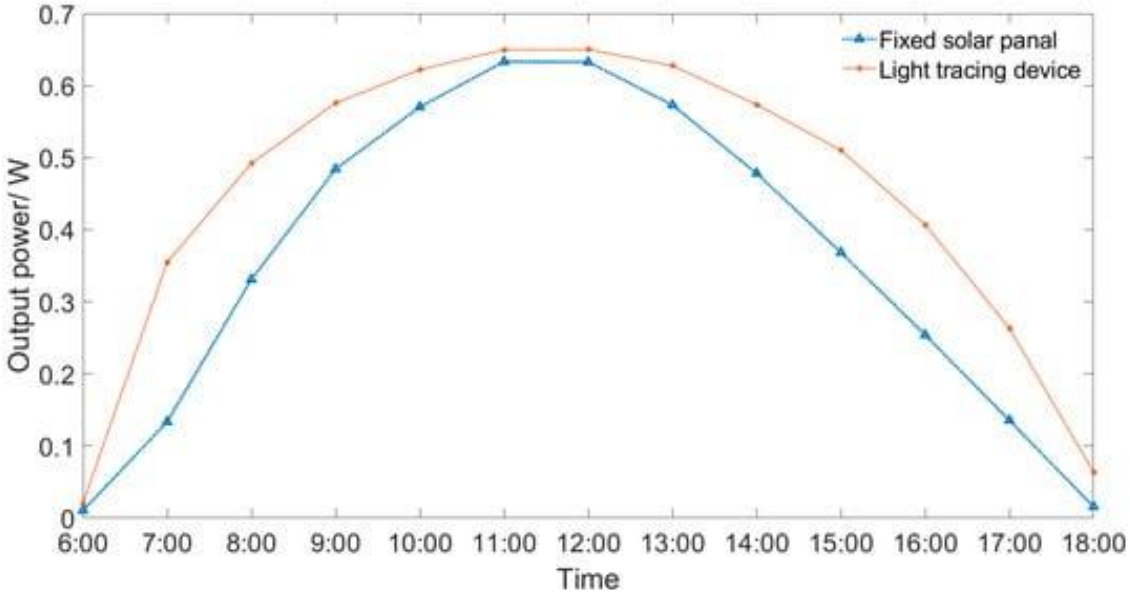

Figure 6. Output power comparison of the two solar panels.

Via multiplication by the time interval, Δt, the experimental solar radiation values $Pi\ tracke$ and $Pi\ fixed$ can be used to express the collected energy, $Wtracked$ and $W\ fixed$, respectively, as follows:

$$W_{tracked} = \sum_{i=0}^{2n} \frac{Pi_{tracked} + Pi+1_{tracked}}{2} \Delta t,$$
$$W_{fixed} = \sum_{i=0}^{2n} \frac{Pi_{fixed} + Pi+1_{fixed}}{2} \Delta t, \quad (19)$$

here the time interval, Δt, is one hour, i.e., 3600 s, and $Pi_{tracked}$ and Pi_{fixed} represent the experimental values of the designed solar tracking system and the fixed solar panel, respectively, at the i-th hour after 6 a.m. For instance, $P°_{tracked}$ and $p°_{fixed}$ are the data for 6 a.m. Since the daytime is, at most, 2n hours, $P_{tracked}^{2n+1}$ and P_{fixed}^{2n+1} are both zero. According to the data in Figure 6, we could calculate that $W_{tracked} 20768.4J$, $W_{fixed} = 16664.4J$, and

$$\frac{W_{tracked} - W_{fixed}}{W_{fixed}} \approx 24.6\%. \quad (20)$$

Comparing the experimental values above with the ideal value predicted in Equation (14), i.e., 26.7%, we could see the agreement of the experimental and theoretical results, which indicates that the proposed device is accurate enough to collect most of the solar energy of an ideal tracker. Considering that the energy consumed by its mechanical system during the tracking of the sun has such a negligible value that it can be omitted, the solar tracking system that we designed and constructed is more efficient in collecting solar energy than the fixed panel.

Compared to the fixed panel, the rough estimations of the extra cost for materials and labor and the extra collected energy of the prototype are CNY 3.98 and 0.4161 kilowatt–hours per year, respectively. Considering the local electricity price, it will take us nearly 14 years to recover the cost. The extra collected energy of the full-scale solar tracker is nearly 100 times that of the prototype, while the extra cost did not increase that much since some components chosen for the prototype, such as the MCU, photoresistors, crystal oscillator, switch, D/A converter, connectors and circuit board, are still available. Additionally, in the case of an industrial product, the price of the materials will be much lower than the estimation above. Taking more materials and motors with higher power into account, it is expected that the extra cost of the full-scale device with the same-sized fixed panel will be 10 times that of the prototype. Therefore, the period for paying back the extra cost of the full-scale device will be significantly reduced to 1.4 years, implying that after that time, the full-sized solar

tracker can be more economical in collecting energy than the full-scale fixed panel.

Conclusions

In this paper, the automatic dual-axis tracking system was designed, developed and implemented. The tracking system design was proposed to accurately adjust the PV module via the primary and secondary axes to follow the sun trajectory using the digital logic design of LDR participations. For this tracker, it employed a pseudo-azimuthal system for good stability of movement mechanism, while the LDRs were utilized and installed using a simple configuration that can reduce tracking errors caused

References

1. Moghaddam, H.A.; Sohrabi, S.N. Designing and Implementing a Location-Based Model to Identify Areas Suitable for Multi-renewable Energy Development for Supplying Electricity to Agricultural Wells. *Renew. Energy* **2022**, *200*, 1251–1264. [Google Scholar] [CrossRef]
2. Hafez, A.Z.; Yousef, A.M.; Harag, N.M. Solar Tracking Systems: Technologies and Trackers Drive Types—A Review. *Renew. Sustain. Energy Rev.* **2018**, *91*, 754–782. [Google Scholar] [CrossRef]
3. Das, M.; Alpina, E.K. Investigation of the Effects of Solar Tracking System on Performance of the Solar Air Dryer. *Renew. Energy* **2021**, *167*, 907–916. [Google Scholar] [Cross Ref]
4. Guney, M.S. Solar Power and Application Methods. *Renew. Sustain. Energy Rev.* **2016**, *57*, 776–785. [Google Scholar] [Cross Ref]
5. Gonzalo, A.P.; Marugan, A.P.; Márquez, F.P.G. A Review of the Application Performances of Concentrated Solar Power Systems. *Appl. Energy* **2019**, *255*, 113893. [Google Scholar] [Cross Ref]
6. Vieira, R.G.; Guerra, F.K.O.M.V.; Vale, M.R.B.G.; Araújo, M.M. Comparative Performance Analysis between Static Solar Panels and Single-Axis Tracking System on a Hot Climate Region Near to the Equator. *Renew. Sustain. Energy Rev.* **2016**, *64*, 672–681. [Google Scholar] [CrossRef]
7. Asadeg, J.; Shopian, K.; Fudholi, A. Performance of Grid-Connected Solar Photovoltaic Power Plants in the Middle East and North Africa. *Int. J. Electr. Compute. Eng.* **2019**, *9*, 3375–3383. [Google Scholar] [CrossRef]
8. Uzun, B.; Onen, A.; Hassanein, H.M.; Mayen, S.M. Rooftop Solar PV Penetration Impacts on Distribution Network and Further Growth Factors—A Comprehensive Review. *Electronics* **2021**, *10*, 55. [Google Scholar] [CrossRef]
9. Quan, S.J.; Li, Q.; Augenbroe, G.; Brown, J.; Yang, P.P. A GIS-based Energy Balance Modeling System for Urban Solar Buildings. *Energy Procedia* **2015**, *75*, 2946–2952. [Google Scholar] [CrossRef]
10. Baljit, S.S.S.; Chan, H.; Sopian, K. Review of Building Integrated Applications of Photovoltaic and Solar Thermal Systems. J. Clean. Prod. 2016, 137, 677–689. [Google Scholar] [CrossRef]
11. Bailek, N.; Bouchouicha, K.; Aoun, N.; EL-Shimy, M.; Jamil, B.; Mostafaeipour, A. Optimized Fixed Tilt for Incident Solar Energy Maximization on Flat Surfaces Located in the Algerian Big South. Sustain. Energy Technol. Assess. 2018, 28, 96–102. [Google Scholar] [CrossRef]
12. Kaddoura, T.O.; Ramli, M.A.M.; AL-Turki, Y.A. On the Estimation of the Optimum Tilt Angle of PV Panel in Saudi Arabia. Renew. Sustain. Energy Rev. 2016, 65, 626–634. [Google Scholar] [CrossRef]
13. Diponkor, B.; Waliullah, G.M.; Hossain, M.A. Design and Implementation of Low Cost Dual Axis Solar Tracking System Using Microcontroller. IITM J. Manag. IT 2021, 12, 88–92. [Google Scholar]
14. Abdollahpour, M.; Golzarian, M.R.; Rohani, A.; Zarchi, H.A. Development of a Machine Vision Dual-Axis Solar Tracking System. Sol. Energy 2018, 169, 136–143. [Google Scholar] [CrossRef]
15. Awasthi, A.; Shukla, A.K.; Manohar, M.S.R.; Dondariya, C.; Shukla, K.N.; Porwal, D.; Richhariya, G. Review on Sun Tracking Technology in Solar PV System. Energy Rep. 2020, 6, 392–405. [Google Scholar] [CrossRef]
16. Lamoureux, A.; Lee, K.; Shlian, M.; Forrest, S.R.; Shtein, M. Dynamic Kirigami Structures for Integrated Solar Tracking. Nat. Commun. 2015, 6, 8092. [Google Scholar] [CrossRef] [PubMed]
17. Poulek, V.; Libra, M. A Very Simple Solar Tracker for Space and Terrestrial Applications. Sol. Energy Mater. Sol. Cells 2000, 60, 99–103. [Google Scholar] [CrossRef]
18. Mavromatakis, F.; Franghiadakis, Y. A Highly Efficient Novel Azimuthal Heliotrope. Sol. Energy 2008, 82, 336–342. [Google Scholar] [CrossRef]
19. Kim, Y.; Han, G.Y.; Seo, T. An Evaluation on Thermal Performance of CPC Solar Collector. Int. Commun. Heat Mass Transf. 2008, 35, 446–457. [Google Scholar] [CrossRef]
20. Kiyak, E.; Gol, G. A Comparison of Fuzzy Logic and PID Controller for a Single-Axis Solar

Tracking System. Renew. Wind Water Sol. 2016, 3, 7. [Google Scholar] [CrossRef]
21. Li, Y.; Chang, K.; Chang, J.; Yu, B.; Liu, L.; Liu, B.; Zhao, X.; Deng, W. Printed Kirigami Organic Photovoltaics for Efficient Solar Tracking. Adv. Funct. Mater. 2022, 32, 2204004. [Google Scholar] [CrossRef]
22. Abdallah, S.; Nijmeh, S. Two Axes Sun Tracking System with PLC Control. Energy Convers. Manag. 2004, 45, 1931–1939. [Google Scholar] [CrossRef]
23. Sungur, C. Multi-Axes Sun-Tracking System with PLC Control for Photovoltaic Panels in Turkey. Renew. Energy 2009, 34, 1119–1125. [Google Scholar] [CrossRef]
24. Kentli, F.; Yilmaz, M. Mathematical Modelling of Two-Axis Photovoltaic System with Improved Efficiency. Elektron. Ir Elektrotechnika 2015, 21, 40–43. [Google Scholar] [CrossRef]
25. Syafii; Nazir, R.; Kamshory; Hadi, M. Improve Dual Axis Solar Tracker Algorithm based on Sunrise and Sunset Position. J. Electr. Syst. 2015, 11, 397–406. [Google Scholar]
26. Skouri, S.; Ali, A.B.H.; Bouadila, S.; Salah, M.B.; Nasrallah, S.B. Design and Construction of Sun Tracking Systems for Solar Parabolic Concentrator Displacement. Renew. Sustain. Energy Rev. 2016, 60, 1419–1429. [Google Scholar] [CrossRef]
27. Laseinde, T.; Ramere, D. Low-Cost Automatic Multi-Axis Solar Tracking System for Performance Improvement in Vertical Support Solar Panels Using Arduino Board. Int. J. Low-Carbon Technol. 2019, 14, 76–82. [Google Scholar] [CrossRef]
28. AL-Rousan, N.; Isa, N.A.M.; Desa, M.K.M.; AL-Najjar, H. Integration of Logistic Regression and Multilayer Perceptron for Intelligent Single and Dual Axis Solar Tracking Systems. Int. J. Intell. Syst. 2021, 36, 5605–5669. [Google Scholar] [CrossRef]
29. Mousazadeh, H.; Keyhani, A.; Javadi, A.; Mobli, H.; Abrinia, K.; Sharif, A. A Review of Principle and Sun-Tracking Methods for Maximizing Solar Systems Output. Renew. Sustain. Energy Rev. 2009, 13, 1800–1818. [Google Scholar] [CrossRef]
30. Radzevich, S.P. Dudley's Handbook of Practical Gear Design and Manufacture, 3rd ed.; CRC Press, Taylor & Francis Group: Boca Raton, FL, USA, 2016; pp. 13–115. [Google Scholar]
31. Johnson, M.A.; Moradi, M.H. PID Control: New Identification and Design Methods, 1st ed.; Ian Kingston Publishing Services: Nottingham, UK, 2005; pp. 1–106. [Google Scholar]
32. Soteris, K. Solar Energy Engineering: Processes and Systems, 1st ed.; Academic Press: San Diego, CA, USA, 2009; pp. 49–120. [Google Scholar]
33. Beling, A.; Xie, X.J.; Campbell, J.C. High-Power, High-Linearity Photodiodes. Optica 2016, 3, 328–338. [Google Scholar] [CrossRef]
34. Tisza, M.; Czinege, I. Comparative Study of the Application of Steels and Aluminium in Lightweight Production of Automotive Parts. Int. J. Lightweight Mater. Manuf. 2018, 1, 229–238. [Google Scholar] [CrossRef]
35. Guo, S.J.; Chen, J.H.; Chiu, C.H. Fuzzy duration forecast model for wind turbine construction project subject to the impact of wind uncertainty. Autom. Constr. 2017, 81, 401–410. [Google Scholar] [CrossRef].